Desalination and Water Treatment
www.deswater.com
32 (2011) 248–255
August
1944-3994 / 1944-3986 © 2011 Desalination Publications. All rights reserved.
doi: 10.5004/dwt.2011.2707

Preparation and characterization of a polysulfone ultrafiltration membrane for bovine serum albumin separation: Effect of polymer concentration

Nora'aini Ali[a]*, S. Hamzah[a], A. Ali[a], A. Endut[b]

[a]*Department of Engineering Science, Faculty of Science and Technology, University Malaysia Terengganu, 21030 Kuala Terengganu, Malaysia*
Tel. +60 (9) 668-3254; Fax +60 (9) 669-4660; email: noraaini@umt.edu.my

[b]*Faculty of Innovative Design and Technology, University Sultan Zainal Abidin, Gong Badak Campus, 21300 Kuala Terengganu, Terengganu, Malaysia*

Received 31 August 2010: Accepted in revised form 17 January 2011

ABSTRACT

This study aimed to investigate the effect of polymer concentration on the morphology and performance of an asymmetric ultrafiltration (UF) membrane for bovine serum albumin (BSA) separation. Flat sheet asymmetric UF membranes were fabricated via dry/wet phase inversion technique. These fabricated membranes were characterized in terms of membrane morphology, membrane pore radius and membrane surface charge. The membrane performance was determined based on pure water flux, sodium chloride rejection and BSA permeation test. Promising results were obtained when BSA rejection ranged from 94.3% to 100%. The optimum membrane in this study was determined by PSF 17% (containing 17 wt% polymer concentration) which successfully exhibited 100% rejection with filtrate flux for about 23.86 L/m^2.h at a pressure of 2 bar. This research also proved that polymer concentration would greatly affect the membrane performance and structural properties, consecutively enhancing the membranes ability for BSA separation.

Keywords: Membrane; Ultrafiltration; Polymer concentration; BSA separation

1. Introduction

Ultrafiltration (UF) is a pressure-driven separation process which walks in the path of development and yet attempting to search for the new quality product through the worldwide. It has a wide variety of applications, ranging from the processing of biological macromolecules, electrocoat paint recovery, enzyme and pharmaceutical preparations to wastewater treatment [1]. In the case of high value therapeutic protein based product, separation and purification costs can be high. Thus, it makes good economic sense to develop cost-effective and scaleable purification processes for such products by using an ultrafiltration membrane in the separation process. During ultrafiltration proteins are separated based on their molecular weight using particular molecular weight cut- off membranes, sometimes moderately different molecular weight proteins are also separated by manipulating the operating conditions [2].

Condition parameters of dope preparation and membrane fabrication provide a significant role in determining a good structure of asymmetric membranes and consequently the membrane performance. Formulation of membrane material and material content greatly influenced the UF membrane at the first stage of membrane-making which was able to alter the membrane morphology, pore size, thickness, molecular weight cut-off, and membrane surface charge [2]. Composition of the polymer in the dope will affect the performance of the resultant membrane as it plays a role in improving

* Corresponding author.

Presented at the Third International Conference on Challenges in Environmental Science & Engineering, CESE-2010 26 September – 1 October 2010, The Sebel, Cairns, Queensland, Australia

This article was originally published with an error in the names of the second and third authors.
This version has been corrected. Please see Corrigendum in vol. 221 (2021) 448 [10.5004/dwt.2021.27422].

macrovoid structure and thickness which influenced the membrane permeability and productivity.

The use of more concentrated polymer has led to the production of a higher concentration of dope at the binodal-phase separation point. Thus, a denser spongious structure will form as well as a lesser possibility of solvent extraction occurring from the surrounding polymer solution to the polymer-lean phase during the formation of the macrovoids. The pore structure of the skin formed on the face in contact with water also changed in the same way. A skin will form at the first instant of the coagulation bath-casting dope contact, and limit the process of diffusion of non-solvent in and solvent out from the layer beneath. As the diffusion rates are much lower at low temperatures, the macrovoids have longer time to grow in size and number according to a nucleation-growth-coalescence process. During the gelling process, the viscoelastic properties of the polymer–solvent gel system control the thickness variation in an originally perfect flat film [3]. When the casting solution comes into contact with the non-solvent in the coagulation bath, a rapid outflow of the solvent from the casting solution to the coagulation bath causes higher-concentration polymer molecules to be aggregated at the top layer [4].

In addition, the solvent ratio also plays an important role along with polymer concentration during membrane formation. The simultaneous adjustment of these two parameters allows for an increase in the viscosity of the dope solution without significant loss in productivity and selectivity [5]. Increase of polymer concentration at a constant solvent ratio produced higher solution viscosity and selectivity but generally lowered the pressure-normalized flux. As well, these condition also affected by the thicker selective skins and transition layers caused by the slower redissolution of initial phase outermost separated regions of nascent membranes from an underlying homogeneous solution during dry phase separation [6].

Polysulfone (PSf) is one of the most extensively applied polymer membrane materials in industry area due to its excellent properties and characteristic including mechanical strength, compaction-resistance, chemical stability and thermal resistance [7]. Due to these special characteristics, PSf can withstand by many types of cleaning methods. Its fairly good chemical resistance was proved its hydrolytic and oxidative stability. PSf is also commercial availability, ease of processing and favorable selectivity-permeability characteristics.

To date, membrane properties have been tailored and adjusted to the specific task in order to enjoy numerous industrial applications with their advantages, including separation and purification of protein molecule. Bovine serum albumin (BSA) is one of the potential proteins which had given a great attention in respect to its role in the pharmaceutical and biotechnology research. Its primary biological function has been associated with its lipid binding properties. This potential protein might reduce the probability of a person acquiring certain diseases, such as insulin dependent diabetes or auto-immune disease. Given the physical and chemical properties of BSA, especially its high molecular weight, it seems quite possible to use ultrafiltration membrane techniques to separate the protein (BSA). In such a situation, ultrafiltration would certainly have an advantage over other techniques [8].

Thus, this study was carried out to investigate the effect of polymer concentration on the performance of asymmetric ultrafiltration membrane protein (BSA) separation. The fabricated membranes were characterized in term of permeability coefficient, membrane morphology, pore radius and membrane zeta potential. The membrane performance has been evaluated based on BSA rejection.

2. Methodology

2.1. Materials

All materials used in this research are of analytical grade. The membranes were fabricated from ternary casting solution which consist of polyrsulfone (supplied by Merck) as polymer, N-methyl-2-pyrrolidone (NMP) (supplied by Merck) as a solvent and water (H_2O) as a non-solvent. BSA (MW = 67,000 Dalton) purchased from Sigma Aldrich has used for the evaluation of membrane performance.

2.2. Membrane preparation

The membranes were prepared using four different ternary dope formulations of casting solutions as shown in Table 1. Asymmetric UF membranes were fabricated via phase-inversion techniques using semi-automated electrical casting machine at an approximately constant shear rate of 200 s^{-1}. Distilled water was used as the first coagulation bath to induce the polymer precipitation for about 24 h. Subsequently, the membrane was immersed in methanol (supplied by Merck) for about 8 h to ensure the excess solvents were totally removed and to strengthen the molecules structure built in the membrane. The membrane was dried at room temperature for 24 h before being used.

Table 1
Ternary dope formulation

PSf (%)	NMP (%)	Water (%)
11	85	4
13	82	5
15	81	4
17	80	3

2.3. Membrane characterization

2.3.1. Permeation with pure water, sodium chloride solution and BSA

All permeation experiments were carried out using dead end cell, supplied by Sterlitech HP4750 with 300 ml processing volume and effective permeation membrane area of 14.6. Distilled water was used for pure water permeation to obtain pure water permeability. Permeation of sodium chloride solution (0.01 M) was done to determine the separation performance of charged solutes. Permeate and feed concentrations of sodium chloride were measured using conductivity meter (Hanna Instruments, Padova, Italy, model HI8633). Based on the sodium chloride rejection, measurement in conjunction with theoretical approaches, the membrane properties were estimated. The steric hindrance pore (SHP) model was employed to deduce the pore size (r_p) and ratio of thickness to porosity ($\Delta x/A_k$) [9].

For the protein permeation test, BSA has been chosen for model protein. For each permeation process, feed pressure was controlled in the range of 2–10 bar by using compressed nitrogen and 10 ml of permeate was collected. The absorbance of feed, permeate and retentate of BSA permeation were analyzed by UV- Vis spectrophotometer (Hitachi U-2000) at a wavelength of 280 nm. The average of three replicates data was reported.

2.3.2. Membrane morphology inspections

The scanning microscopy electron (SEM) (JSM P/N HP475 model) has been used to inspect the morphology of in house fabricated membrane. An automatic coater JFC 100 model has used to coat the membrane specimen. For this purpose, the membrane samples were fractured in liquid nitrogen and sputtered with gold, before transferring them under the microscope.

2.3.3. Zeta potential measurementl

Zeta potential was measured using an electrokinetic analyzer (EKA) (Anton Paar Gmbh Graz, Austria). The conductivity dip-in-cell was calibrated before used and the membrane sheets were cut into a rectangular size (12.8 cm × 5.1 cm) that mounts on the measuring cell. EKA was rinsed with deionized water before measurement of zeta potential to remove the bubbles from the sample. After measurement, the results were analyzed using Visiolab software.

2.3.4. Theoretical approach

In order to determine the membranes pore radius, the data were obtained from the permeation experiments of four membranes with varying the polymer concentration and shear rates. The coefficient η was estimated where a simple estimation of the pore radius can be obtained by considering the uniform pore size distribution of the membrane and it is expressed as a simple analytical function of η below:

$$\eta = 1 - \frac{2(1-R)}{2-R} \tag{1}$$

The membrane parameters λ, σ, H_F, H_D, S_F and S_D were determined. The H_F and H_D parameters are for steric hindrance and frictional forces that impede convective and frictional forces that impede convective and diffusive transport, respectively are expressed by the SHP model as in Eqs. (2)–(6).

$$H_F = 1 + \frac{16\eta^2}{9} \tag{2}$$

$$S_D = \left(1-\eta^2\right) \tag{3}$$

$$S_F = \left(1-\eta^2\right)\left[2-\left(1-\eta^2\right)\right] \tag{4}$$

$$\sigma = 1 - H_F S_F \tag{5}$$

$$P_s = \frac{(1-\sigma)J_v}{\ln F} \tag{6}$$

The membrane porosity (Δ*K*) can be deducted based on Eq. (7) where $P_s = D_s/\Delta x$ and D_s is defined as a diffusion coefficient (1.61×10^{-9} m²/s) whose H_D equal to 1 [9].

$$P_s = H_D S_D D_s \left(\Delta K/\Delta x\right) \tag{7}$$

Then, the pore radius (r_p) can be determined where η is defined as the ratio of solute radius (r_s) to pore radius (r_p).

$$\eta = \frac{r_s}{r_p} \tag{8}$$

3. Results and discussion

3.1. Pure water permeability

The membrane permeation test for pure water flux was first measured in order to determine the stability and porosity of the UF membranes used. It depends on permeability coefficient, in which higher the permeability, the more porous membrane will be. Fig. 1 represents the pure water flux vs. pressure of four in-house fabricated membranes with different polymer concentrations.

All membranes show a linear function for increase of applied pressure from 2 to 10 bar and this profile was followed the Hagen–Poiseuille equation which stated that water flux incensement is proportional to the increased of applied pressure.

$$J = \left(\varepsilon r^2 \times \Delta P\right)/8\eta'\tau\cdot\Delta x \tag{9}$$

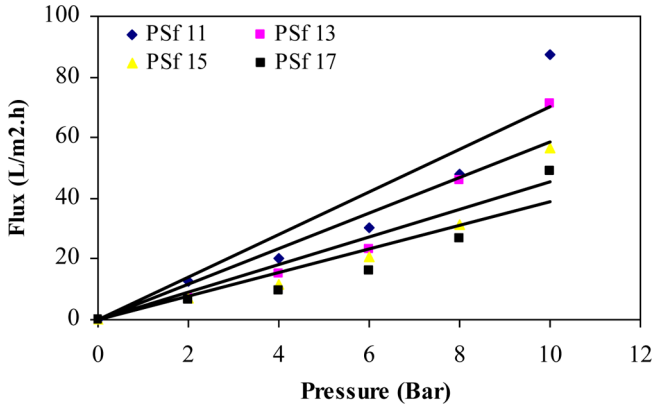

Fig. 1. Pure water flux of four membranes with different polymer oncentrations. PSf 11 ($y = 7.0195x$, $R^2 = 0.8388$), PSf 13 ($y = 5.8681x$, $R^2 = 0.8582$), PSf 15 ($y = 4.5413x$, $R^2 = 0.8472$) and PSf 17 ($y = 3.8741x$, $R^2 = 0.8260$).

J is defined as the water flux through the membrane at a driving force of $\Delta P/\Delta x$, with ΔP being the pressure difference (N/m^2) and Δx the membrane thickness (m). The proportionality factor contains the pore radius, r (m), the liquid viscosity, ή (P.a.s), the surface porosity of the membrane, ε (= $n\pi r^2$/surface area) and the tortuosity factor, τ.

Table 2 shows the permeability coefficient of four fabricated membranes. PSf 11 membrane shows the greatest permeability coefficient which was 7.02 L/m^2.h.bar and the permeability coefficient decreased with increased polymer concentration in the membrane solution. The results of pure water flux measurement also represent the hydraulic permeability of membranes which is the property that depends on the membrane thickness and porosity. Increase of the polymer concentrations tends to increase the membrane thickness and the membrane becomes denser, which consequently results in lower hydraulic permeability as can be seen in PSf 17. This finding can be supported by the SEM morphology where the membranes with higher polymer concentrations present a denser structure.

The comparison between the in-house fabricated membranes and commercial UF membranes in terms of permeability rates is shown in Table 3. These results postulate that the fabricated membranes have similar potential as that of commercial UF membranes.

3.2. NaCl rejection measurement

Figs. 2a and 2b show the flux and rejection of sodium chloride by employing the four types of PSf membranes with different polymer concentrations.

According to the experimental data for all membranes, the fluxes and rejection increased as the pressure increased and the trend of salt rejections decreased in the following manner: PSf 17 > PSf 15 >PSf 13 > PSf 11. PSf

Table 2
Permeability coefficient of membranes with different polymer concentrations

Membrane ID	Polymer concentration (%)	Permeability coefficient (L/m^2.h.bar)
PSf 11	11	7.02
PSf 13	13	5.87
PSf 15	15	4.54
PSf 17	17	3.87

Table 3
Summary of the permeability rates of commercial UF membranes and fabricated membranes*

Membranes	Permeability (L/m^2.h.bar)
Maximum	6.07
Mean	4.96
Minimum	3.81
11%PSf*	7.02
13%PSf*	5.87
15%PSf*	4.54
17%PSf*	3.87

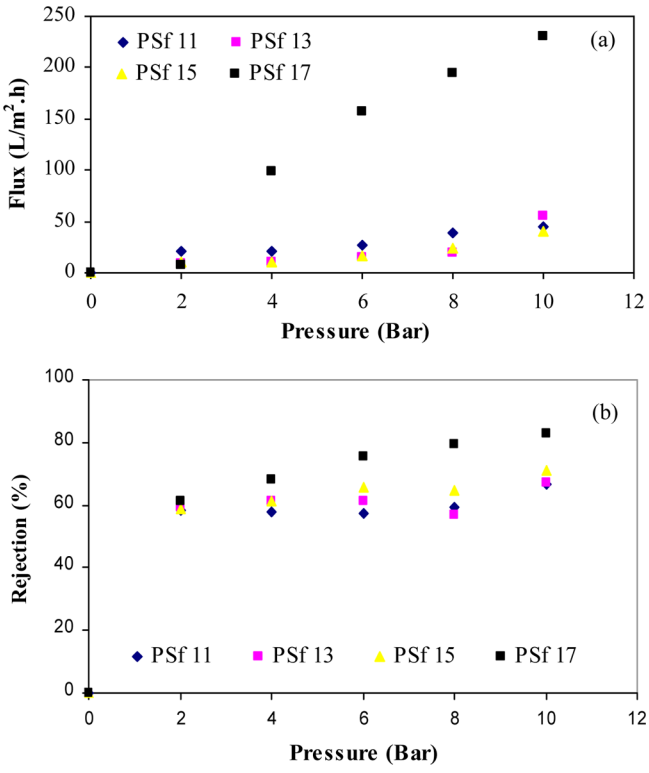

Fig. 2. (a) Fluxes and (b) sodium chloride rejection using four types of membranes with different polymer concentrations.

17 exhibited the highest percentage NaCl rejection for about 83% with applied pressure of 10 bar. This observation agrees with the findings in [6] where the increase of polymer concentration increased the solute rejections since high dope viscosity tends to promote a more selective membrane.

3.3. Modelling result

The steric hindrance pore (SHP) model is a rigorous approach to describe the membrane properties in terms of the pore radius. This model has been extensively used to explain the transport mechanism in UF membranes considering the pore radius effects for the permeation of sodium chloride [10]. A statistical analysis of experimental data with different polymer concentration membranes is presented in Tables 4 and 5.

According to the SHP model, diffusion and convection factors parameters contributed significantly to the membrane transport mechanism for the ultrafiltration process. Separation of electrolytes which contained different charge ions have different signs and valences that can be manipulated according to the rejection differences by the membranes. From this theoretical approach, it was found that the reflection coefficients strongly influenced the membrane performances which were discussed in terms of selectivity (percentage of ion chloride rejection), productivity (fluxes) and membranes pore radius.

According to Figs. 3 and 4, membrane pore radius decreased as polymer concentrations increased, consequently trimmed down the flux of sodium chloride permeation

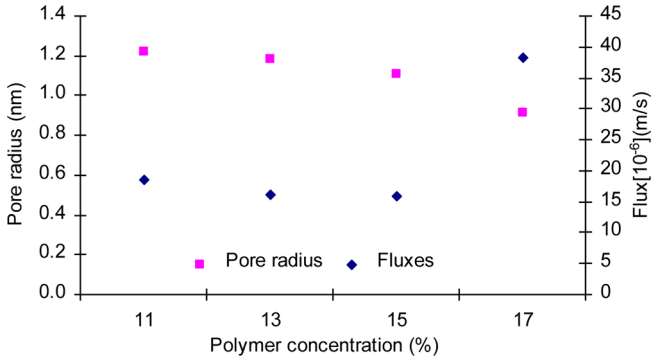

Fig. 3. Pore radius and fluxes vs. different polymer concentrations.

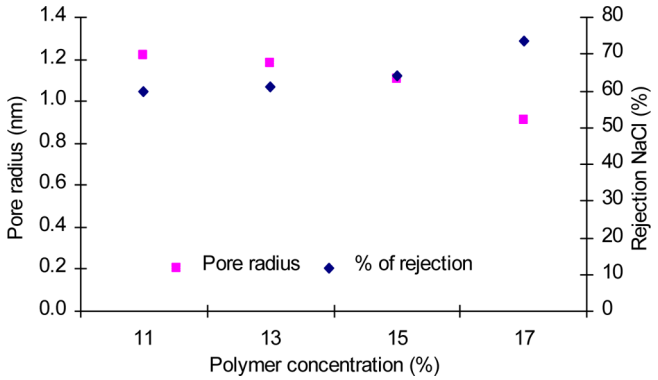

Fig. 4. Pore radius and percentage of rejection NaCl vs. different polymer concentrations.

Table 4
Numerical results and diffusion parameter at different polymer concentrations

Membranes ID	Ratio of solute radius (η)	Stearic parameters under diffusion (H_F)	Distribution coefficient under convection (S_D)	Distribution coefficient under diffusion (S_F)	Reflection coefficient (σ)
PSf 11	0.43	1.33	0.33	0.55	0.28
PSf 13	0.44	1.35	0.31	0.53	0.29
PSf 15	0.47	1.40	0.28	0.48	0.34
PSf 17	0.59	1.63	0.18	0.32	0.50

Table 5
The modeling results; values of P_S, Δx, A_K, r_p and $\Delta x/A_K$ at different polymer concentrations

Membrane	Solute permeability (P_S) [×10⁷] (m/s)	Effective membrane thickness (Δx) [×10⁻⁵] (m)	Membrane porosity (A_K)	Pore radius (r_p) (nm)	$\Delta x/A_K$ [×10⁻⁵]
PSf 11	5.22	3.33	3.09		1.22
PSf 13	2.37	16.12	3.25	1.18	5.28
PSf 15	3.20	5.93	3.71	1.11	1.74
PSf 17	13.95	3.16	6.86	0.91	0.86

for PSf 11, PSf 13 and PSf 15. However, contradicted with the other membranes, PSf 17 was promoted the highest flux incensement even it was prepared using the highest polymer concentration. From the depicted graph, it can also be found that sodium chloride rejections increased with increasing of polymer concentration and the results of the theoretical approach revealed that the membrane with 17% of PSf concentration indicated the smallest pore radius compare to the other membranes.

Overall view of the results shows that the rejection of BSA exhibited the high percentage of rejection with PSf 17 where totally BSA were rejected at pressures of 2 and 4 bar. It is supported with the correlation between the rejection and flux of BSA (as discussed before) where membrane with PSf 17 promoting the highest rejection. According to Knoll and Hermans [11], the solute radius of BSA is 3.5 nm and from the result of BSA separation, it supposedly can promote a high separation of BSA, feasible to the membrane where the solute radius, rs of BSA is larger than the membrane pore radius. The result for the average of the membrane pore radius and BSA rejection are tabulated in Table 6. It clearly shows that the in-house fabricated membrane with high polymer concentration have a high potential of BSA separation with the r_s BSA > r_p membrane. This result postulated that a membrane with PSf 17 can be considered as a superior membrane due to the trade-off between the moderate flux and high rejection percentage in order of predicting the best condition of the fabrication with high performances membranes.

Table 6
BSA rejection at different polymer concentrations

Polymer concentration (%)	Average pore radius, r_p (nm)	Average rejection of BSA (%)
11	1.22	96.86
13	1.18	97.87
15	1.11	99.17
17	0.91	99.53

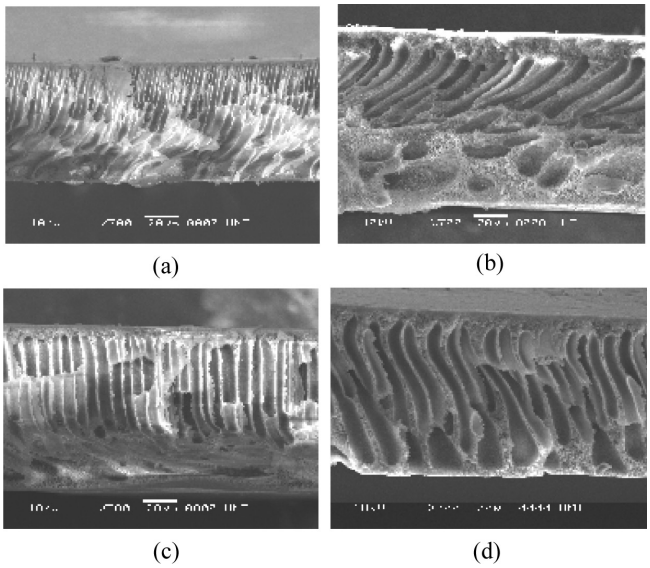

Fig. 5. Cross section of PSf membrane at different polymer concentrations: (a) PSf 11 (b) PSf 13 (c) PSf 15 (d) PSf 17.

3.4. Membrane morphology

In this study, all the prepared membranes show an asymmetric structure which comprised two layers; skin active layer and supporting layer. Both layers had a significant role in the membrane transport property. The cross-section morphology of UF membranes observed by SEM is shown in Fig. 5. Exception to the PSF 17, all the prepared membranes are porous due to its regular finger voids structure [12].

From the observation, increase of the polymer concentration was greatly affected the morphology and membrane structure since it can induce transformation from thinner to thicker skin [6]. PSf 11 and PSf 13 membranes comprised a large macroporous finger like structure. This membrane comprises a skin layer that is well developed and supported by a porous support layer with large finger-like, sponge-like and macrovoid structures. This is due to the solvent–non-solvent exchange, leading to the different starting conditions for phase separation at layers far from the surface.

PSf 15 membrane also shows a large microporous finger-like structure which indicates that this membrane possesses a high porosity. At a lower polymer concentration, non-solvent concentration in the dope solution was higher. Therefore, the non-solvent diffusion into the membrane was higher and the phase separation velocity led to the formation of big finger-like pores in the membranes as can be seen in this type of membrane. Besides, lower polymer concentration membranes exhibited a few sponge structures which resulted from the rapid solvent precipitation during phase inversion process [13]. Separation behavior occurs at the skin (active) layer of the membrane and the bottom layer (support layer) acts as a mechanical strength of the membrane.

PSf 17 membrane presents the densest skin layer compared to the other fabricated membranes. It displays a tiny and micropore finger-like structure with fine tuned arrangement. PSf 17 consists of high polymer concentration which enhanced the viscosity of dope, leading to the formation of a smaller pore size. This phenomenon occurs since high viscosity would avoid the diffusion exchange rate of solvent and non-solvent in a sub-layer inducing fast phase separation at the skin layer and slowing the precipitation rate of the sub-layer. Hence, this resulted

in the formation of an asymmetric membrane with a dense and thick skin layer, supported by a closed cell sub-layer These substructures have a good impact on separation mechanism especially for large molecular weight of BSA molecules which also can be seen through the surface layer where the BSA was totally rejected with these membranes.

3.5. Membrane zeta potential

The membrane surface charge is expressed with zeta potential (ZP) value and the ranges of ZP for in-house fabricated membranes are presented in Table 7. PSf 17 shows the widest range and highest ZP values compared to other membranes. All the membrane surfaces were negatively charged as it was influenced by the character of PSf polymer which poses negative charge on sulfate ion. Increase in polymer concentration has produced a membrane that has a wide range of membrane surface charge distribution and this has allowed the membrane to perform with high selectivity as it manages to perform almost 100% rejection of BSA. Hinke and Staude [14] showed that the range of ZP value obtained for each membrane measured is likely due to the ratio of the pore radius to the double layer thickness. The strong deviations of zeta potential values were usually justified by differences in the membrane surface charge and the electrokinetic measurements. Hydrodynamic conditions inside the cell, for example, the channel height and the electrical data reliability, which is related to the electrodes location, may affect the ZP values [15].

3.6. Separation performance of BSA single solution

An ideal protein separation process must combine high productivity and selectivity of separation with feasible at mild operating conditions. The results of BSA and flux rejection for each polymer concentration membranes are illustrated in Figs. 6 and 7. The highest flux obtained was at 94.84L/m^{2}h via permeation of PSf 15 at an optimum pressure of 10 bar. In this research, the filtrate fluxes of all membranes present the same trend; flux increased when the applied pressure increased.

The rejection of BSA with different polymer concentrations was not lined up in the same trend since the rejection inconsistently increased and decreased. However, promising results were obtained when the rejection of BSA ranged from 94 to 100%. The inconsistent trend of BSA rejection might be affected by concentration polarization and membrane fouling which result from the adsorption or deposition on the external membrane surface, or due to adsorption or deposition within the pores [16]. In this case, BSA was rejected on the membrane surface and tended to form a cake layer and also mighy get adsorbed on the membrane surface due to electrostatic adsorption or hydrophobic interaction.

During the membrane separation, BSA dissolved in the solution, was convectively driven to the membrane surface where they built up a concentration polarization boundary layer near the membrane surface. This phenomenon resulted in increasing the concentration of dissolved BSA near the membrane surface. Owing to this effect, the mobility of the molecule also decreased, which led to a more profound concentration polarization on the membrane surface, the rejection of BSA declined.

Overall view of the results proved that PSf 17 membrane showed the highest rejection of BSA, for about 100% rejection at an optimum pressure of 2 bar. This protein

Table 7
Range of zeta potential of different membranes

Membrane ID	Range of zeta potential (mV)
PSf 11	–7.9 to –11.4
PSf 13	–8.1 to –10.3
PSf 15	–6.9 to –10.8
PSf 17	–6.8 to –12.3

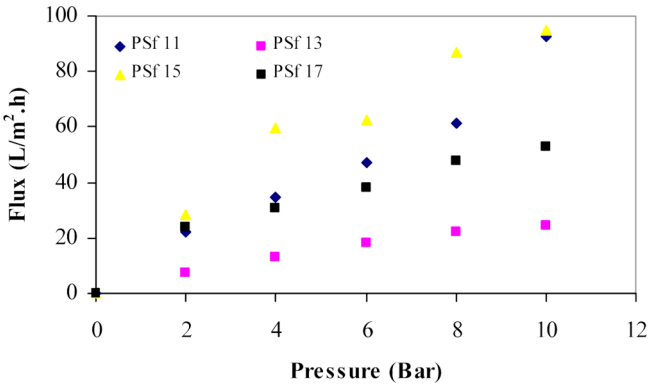

Fig. 6. Filtrate flux of BSA separation.

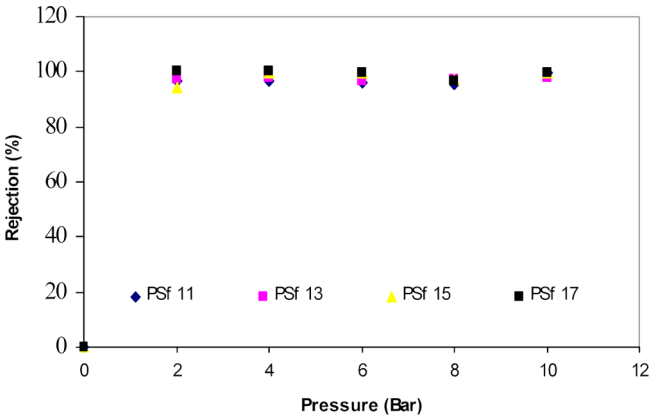

Fig. 7. BSA rejection using membranes with different polymer concentrations.

could be retained by PSF 17 membranes sufficiently due to the large MW of BSA (67 kDa). A dramatic increased in protein rejection with a high polymer concentration membrane was also due to the strong electrostatic repulsion of the negatively charged protein from the membrane pores. Regarding their charge repulsion, BSA was easily rejected and did not transmit through the pores close to the size of the protein with a similar charge. Charged protein is normally difficult to penetrate the membrane, thus it gained transmission through the membrane due to the shielding of charges. This shielding effect reduces the hydrodynamic diameter of a protein differing from its isoelectric point and also naturally decreases the charge of the membrane [17].

4. Conclusions

Asymmetric polysulfone ultrafiltration membranes with different polymer concentrations were successfully developed via a simple dry/wet phase inversion technique. The findings of this study proved that the polymer concentration greatly influenced the membrane performance, morphology and membrane zeta potential. Increase of the polymer concentration tends to reduce the membrane pore size, consequently promoting the highest rejection of protein BSA. Based on the experimental data, PSf 17 membrane seemed to be an optimum membrane in this study in showing an outstanding performance of BSA separation.

Acknowledgements

The authors wish to express their sincere gratitude to the undergraduate student Suriyani Abd. Rahman from Engineering Science Department, Universiti Malaysia Terengganu, for her contributions to obtain part of experimental data for this study.

References

[1] R. Ghosh, Review: Protein separation using membrane chromatography: opportunities and challenges. J. Chromatography A, 952 (2002) 13–27.
[2] R. Ghosh and Z.F. Cui, Protein purification by ultrafiltration with pre-treated membrane. J. Membr. Sci., 167 (2000) 47–53.
[3] J.F. Blanco, J. Sublet, Q.T. Nguyen and P. Schaetzel, Formation and morphology studies of different polysulfones-based membranes made by wet phase inversion process. J. Membr. Sci., 283 (2006) 27–37.
[4] B. Chakrabarty, A.K. Ghoshal and M.K. Purkait, Preparation, characterization and performance studies of polysulfone membranes using PVP as an additive. J. Membr. Sci., 315 (2008) 36–47.
[5] A.L. Ahmad, M. Sarif and S. Ismail, Development of an integrally skinned ultrafiltration membrane for wastewater treatment: effect of different formulations of PSf/NMP/PVP on flux and rejection. Desalination, 179 (2005) 257–263.
[6] Y. Yang and P. Wang, Preparation and characterizations of a new PS/TiO_2 hybrid membranes by sol–gel process. Polymer, 47 (2006) 2683–2688.
[7] Y. Wan, J. Lu and Z. Cui, Separation of lysozyme from chicken egg white using ultrafiltration. Separ. Purif. Technol., 48 (2006) 133–142.
[8] A.R. Hassan, A. Nora'aini, A. Norhidayah and A.F. Ismail, A theoretical approach on membrane characterization: the deduction of fine structural details of asymmetric nanofiltration. Desalination, 206 (2007) 107–126.
[9] A.F. Ismail and A.R. Hassan, The deduction of fine structural details of asymmetric nanofiltration membranes using theoretical models. J. Membr. Sci., 231 (2003) 25–36.
[10] D. Knoll and J. Hermans, Polymer protein interaction: Comparison of experiment and excluded volume theory. J. Biol. Chem., 258 (1993) 5710–5715.
[11] P.J. Brown, S. Ying and J. Yang, Morphological structure of Polyetherketone membranes for gas separation prepared by phase inversion. AUTEX Res. J., 2 (2002) 101–108.
[12] T.H. Young and L.W. Chen, Pore formation mechanisms of membranes from phase inversion process. Desalination, 103 (1995) 233–247.
[13] E. Hinke and E. Staude, Streaming potential of microporous membranes made from homogeneously functionalized polysulfone. J. Appl. Polym. Sci., 42 (1991) 2951–2958.
[14] A.I. Cavaco Morão, A.M. Brites Alves and M.D. Afonso, Concentration of clavulanic acid broths: Influence of the membrane surface charge density on NF operation. J. Membr. Sci., 281 (2006) 417–428.
[15] M. Feins and K.K. Sirkar, Novel integrally staged ultrafiltration for protein purification. J. Membr. Sci., 248 (2005) 137–148.
[16] M.M.D. Zulkali, A.L. Ahmad and C.J.C. Derek, Membrane application in proteomic studies: Preliminary studies on the effect of pH, ionic strength and pressure on protein fractionation. Desalination, 179 (2005) 381–390.